Nonlinear Dyn
https://doi.org/10.1007/s11071-019-04838-5

ORIGINAL PAPER

The coupling strength versus convergence speed in pinning control

Ming-Yang Zhou · Xiao-Yu Li · Wen-Man Xiong · Hao Liao

Received: 9 July 2018 / Accepted: 12 February 2019

Abstract Pinning control, which drives a networked system to a coherent state, has attracted much attention in recent years. The controllability of pinning control is usually characterized by the ratio of the largest to the smallest eigenvalues of the Laplacian relevant matrices. In this paper, we demonstrate that the ratio evaluation cannot precisely characterize the pinning controllability, especially the convergence rate (Lyapunov exponent) of a system. Thus, we propose a method to the pinning controllability from two perspectives: the coupling range and convergence speed. The former represents the synchronization range of the coupling strength between agents. Higher coupling range is better. However, the convergence speed characterizes the convergence rate of the pinning synchronization. Moreover, we analytically show that the classical ratio metric, the coupling range and convergence speed cannot arrive at optimums simultaneously. Comparing with the classical ratio metric, the pinning controllability could be better characterized by the coupling range and convergence speed in analytical and practical ways.

M.-Y. Zhou (✉) · X.-Y. Li · W.-M. Xiong · H. Liao
College of Computer Science and Software Engineering, Shenzhen University, Shenzhen 518060, People's Republic of China
e-mail: zhoumy2010@gmail.com

X.-Y. Li
e-mail: 2172272042@email.szu.edu.cn

H. Liao
e-mail: jamesliao520@gmail.com

Published online: 06 April 2019

Keywords Pinning control · Synchronization · Control strength · Convergence speed

1 Introduction

A large variety of natural systems could be represented by complex networks in which nodes describe agents of the system and edges describe the interaction between agents, including biology systems, social networks and so on [1,2]. Individuals of these systems exchange information merely with their neighbors, and the whole agents of the system may arrive at a coherent state if the coupling strength between agents satisfies some criteria [3,4]. In order to control the collective dynamics of the networks, instead of directly controlling every node, we only require to drive a small fraction of nodes [3,5]. For example, when a swarm flies to a new nest site, only the scouts (%5 bees) know the direction that the swarm must fly. The small fraction of bees could guide the swarm right to the new home in the majority of cases [1]. Analyzing the underlying mechanism of the natural systems may help us better design man-made systems, such as wireless sensors and unmanned aerial vehicles [6–8]. Pinning control, which drives the system to a synchronized state by injecting feedback gains into a small number of nodes, provides convenient access to model the natural systems introduced above.

The dynamics of a pinning networked system is determined by three aspects: dynamics of a single node,

network topology and the control strategies. Pecora and Carroll [4] investigated the general relationship between synchronization and network topology and introduced the synchronization condition for complex networks, based on which the criterion of the pinning controllability was established [2,9,10]. According to the traditional control theory, the pinning controllability is usually characterized by the ratio of the largest to the smallest eigenvalues of the networks' Laplacian relevant matrices [11,12]. The ratio criterion supplies the sufficient condition to guarantee the control of pinning networked systems. Then, much effort was devoted to investigating the influence of various factors on the ratio condition [13], including the time delay [14,15], nodal dynamics [16,17], network structures [18,19] and so on [9,20,21].

In practice, we usually desire to increase our ability to control a network, i.e., increasing the strength of pinning controllability (control strength for short). Then, a variety of control strategies were devised to increase the control strength. For example, He et al. [22,23] use impulse control to drive nonlinear multi-agent systems. Lei et al. [24–26] investigate the adaptive control in synchronization systems. Besides, fast-switching control [27,28] and other strategies [29] are also introduced into the field of pinning control. Among these researches, many works investigate the relationship between controllability and network structure. Since many networks from diverse fields follow similar structures, such as power-law degree distribution, small-world phenomenon, community structure and so on [30,31], a natural problem arises that whether we can find an universal method to identify the influential pinning nodes only based on network topology [3,32]. The problem is rephrased of finding a fixed number of candidate nodes to maximize the ratio criterion introduced above. However, identifying the optimal set of pinning nodes is an NP-hard problem. Hence, an alternative solution is to use efficient heuristic methods [33,34], including degree, betweenness, PageRank, closeness, K-shell and other local and global ranking metrics [35,36]. Among these researches, Wang et al. [37] show that the high-degree method performs well in random networks, yet fails in many real networks. Betweenness outperforms high-degree method in US airline network and the protein–protein network in yeast, but requires high time complexity [38]. Accordingly, Jalili et al. [39] apply differential evolution to choose the optimal drivers. Moreover, Orouskhani et al. [40] find that the locations of the optimal drivers are also associated with the feedback gains of each node, and they utilize the swarm optimization technique to determine the locations and the feedback gains of the driver nodes. Recently, Amani et al. [18] introduce matrix perturbation method into the detection of influential nodes and increase the strength of the pinning controllability much. However, most previous works aim to increase the controllability of the ratio metric. The problem of whether the ratio metric can precisely characterize the pinning controllability lacks in-depth analysis.

In the paper, we investigate the fundamental problem of how the ratio metric fails in precisely characterizing the master stability function (MSF) of pinning control systems. In pinning control, we usually concern the candidate range of the coupling strength to guarantee synchronization and the convergence rate of the pinning synchronization. However, the theoretical results show that the classical ratio metric only roughly evaluates the pinning controllability, lacking high precision. To solve the drawback of the ratio metric, we characterize the pinning controllability from the coupling range and convergence speed. The two parts describe the pinning synchronization from entirely different perspectives: the range of the coupling strength between agents and the convergence rate of the pinning synchronization. A wider range of the coupling strength means it is easier to tune the coupling parameter between nodes in engineering, while a higher convergence rate means a higher Lyapunov exponent in pinning control. Then, we use the differential evolution method to optimize the three metrics (the classical ratio metric, coupling range and convergence speed), and the experiments show that real networks cannot reach the optimums of the three metrics simultaneously. Thus, the classical ratio metric cannot precisely characterize the pinning controllability. The proposed coupling range and convergence speed provide two better metrics to evaluate pinning controllability.

The organization of the paper is as follows: In Sect. 2, we describe the pinning control problem and introduce the proposed coupling range and convergence speed. In Sect. 3, we compare the experimental performances of the classical ratio evaluation, coupling range and convergence speed. At last, the conclusion is drawn in Sect. 4.

2 Materials and methods

In the section, we first use an example to show the drawback of the classical ratio metric in Sect. 2.1 and describe the pinning control problem in Sect. 2.2. We then introduce the proposed coupling range and convergence speed in Sect. 2.3. The theoretical difference among the classical ratio metric, coupling range and convergence speed is presented in 2.4.

2.1 An example of ratio metric, coupling range and convergence speed

Figure 1 shows an example of the drawback of the classical ratio metric. We construct an artificial network that has 11 nodes and 24 edges (see the network structure in Fig. 1a, respectively). The settings of the nodal dynamics and feedback strength are shown in Sect. 3.2. We use brute force method to choose three optimal pinning nodes according to the ratio metric R, the range of coupling strength ω and the convergence speed v, respectively, and get different optimal sets of pinning nodes (See panels a–c in Fig. 1). The results show that the optimal sets of pinning nodes of the three metrics have the different Lyapunov exponents in Fig. 1d. Further, we show the ratio metric R, the range ω of the coupling strength and convergence speed v of optimal pinning node sets that correspond to the three metrics, respectively, in Fig. 1e. Interestingly, optimizing the classical ratio metric cannot guarantee the control of the dynamics since $v = 0.0174 > 0$ in panel Fig. 1e. Here, $v > 0$ means positive Lyapunov exponent, implying that the system is chaotic and cannot converge to a stationary state. Moreover, the optimal R also cannot arrive at the largest range of the coupling strength (see Fig. 1e). Thus, the classical ratio metric R cannot precisely characterize the pinning controllability.

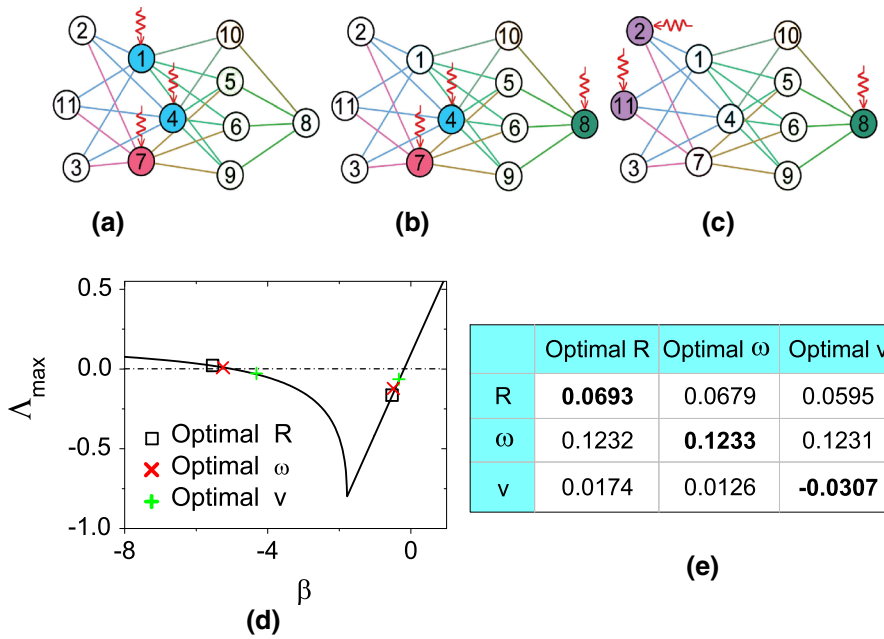

	Optimal R	Optimal ω	Optimal v
R	**0.0693**	0.0679	0.0595
ω	0.1232	**0.1233**	0.1231
v	0.0174	0.0126	**-0.0307**

(e)

Fig. 1 The schematic illustration of the differences among ratio metric R, the range ω of the coupling strength and convergence speed v of pinning control. Colored nodes are pinning nodes. **a** The three pinning nodes corresponding to the optimal R. **b** The three pinning nodes corresponding to the optimal range ω of the coupling strength. **c** The three pinning nodes corresponding to the optimal convergence speed v. **d** The Lyapunov exponent $\Lambda_{\max}$ [see Eq. (11)] as a function of $\beta = c\lambda_i$ (see Eq. 4) that corresponds to the three metrics, respectively. The smaller $\Lambda_{\max}$ is better. **e** The performances of different optimal sets of pinning nodes. For each column, we first obtain the optimal set of pinning nodes by optimizing R (or ω, v), and then calculate the R, ω and v of the nodes set

2.2 The definition of pinning control

We first introduce some notations and concepts used throughout this paper. We model a multi-agent system by a network $G = (V, E)$ with nodes $V = (1, 2, \ldots, N)$ representing agents, and edges $E \subseteq V \times V$ representing the connections between agents [41]. Here, edges are treated as undirected and unweighted, which is possible in some cases, for example, in sensor networks, two sensors either have full-duplex wireless connections, or not. Denote the set of neighbors of node i as $N_i = \{j|(i, j) \in E\}$. Network G is represented by a symmetric adjacent matrix $A = (a_{ij})_{N\times N}$, where $a_{ij} = a_{ji} = 1$ if $(i, j) \in E$; otherwise, $a_{ij} = a_{ji} = 0$. Laplacian matrix of G is defined as $L = (l_{ij})_{N\times N}$, where $l_{ii} = \sum_{j,j\neq i} a_{ij}$, and $l_{ij} = -a_{ij}, i \neq j$. Elements on the diagonal of L are the degree d_i of node i [41,42].

Consider an undirected network containing N identical linearly and diffusively coupled nodes, with each node being a z-dimensional dynamical system. The state equations of the whole nodes are [4]

$$\dot{\mathbf{x}}_i = f(\mathbf{x}_i) - c\sum_{j=1}^{N} l_{ij} H\mathbf{x}_j, \quad i = 1, 2, \ldots, N, \tag{1}$$

where $\mathbf{x}_i = (x_{i1}, x_{i2}, \ldots, x_{iz})_z^T$ is the state variable of node i, the constant c indicates the coupling strength between nodes, and $H = (h_{ij})_{z\times z}$ is a matrix coupling different variables.

Supposing that we inject feedback gains into a small set of nodes $(i_1, i_2, \ldots, i_m)$, the dynamics of these pinning nodes should be modified as [3,37,43]

$$\dot{\mathbf{x}}_{i_k} = f(\mathbf{x}_{i_k}) - c\sum_{j=1}^{N} l_{i_k j} H\mathbf{x}_j - cd(\mathbf{x}_{i_k} - \bar{\mathbf{x}}), \quad k = 1, 2, \ldots, m, \tag{2}$$

where d and $\bar{\mathbf{x}}$ are the feedback strength and the stationary state. $\bar{\mathbf{x}}$ should subject to $\dot{\bar{\mathbf{x}}} = f(\bar{\mathbf{x}})$.

To assess the stability of the system, we diagonalize the variational equations of Eqs. (1) and (2) into [44]

$$\dot{\xi}_i = [Df + c\lambda_i H^T]\xi_i, \quad i = 1, 2, \ldots, N, \tag{3}$$

where Df is the Jacobian matrix of f, and ξ_i is the state variables linearly transferred from the variational states $\mathbf{x}_i$. λ_i are the eigenvalues of $-L - D$ $(0 > \lambda_1 \geq \lambda_2 \geq \ldots \geq \lambda_N)$, and D is a diagonal matrix with $D_{ii} = d$ if node i is a pinning node; otherwise, $D_{ii} = 0$.

The stability of Eqs. (1) and (2) is equivalent to that of Eq. (3). To stabilize Eq. (3), the perturbations transverse to the synchronization manifold should be damped, i.e., $\lambda_{\max}(Df + c\lambda_i H^T) < 0, \forall i = 1, 2, \ldots, N$.

Now, we only concern the associated generic master stability function

$$\dot{\zeta} = [Df + \beta H^T]\zeta. \tag{4}$$

Supposing that the stabilization manifold of Eq. (4) is $\beta \in (\alpha_1, \alpha_2)$. Accordingly, for Eq. (3), we should guarantee $\alpha_1 < c\lambda_i < \alpha_2, i = 1, 2, \ldots, N$. The stabilization manifolds could be divided into three classes [3,4]:

Case 1 The manifold is $\beta \in S1 = (-\infty, \alpha_1)$, where α_1 is a real negative number. To ensure the synchronization, we obtain

$$c\lambda_1 < \alpha_1. \tag{5}$$

Therefore, the synchronization strength of the system could be characterized by λ_1 in this case. Smaller λ_1 is better.

Case 2 The manifold is $\beta \in S2 = (\alpha_1, \alpha_2)$, where α_1 and α_2 are real numbers $(\alpha_1 < \alpha_2 < 0)$. The stabilization condition is

$$\alpha_1 < c\lambda_N, \quad c\lambda_1 < \alpha_2. \tag{6}$$

This can be simplified as

$$R = \frac{\lambda_1}{\lambda_N} > \frac{\alpha_2}{\alpha_1}. \tag{7}$$

Increasing R would increase the pinning controllability, and therefore, higher R is better. In fact, R is the widely accepted metric to characterize the pinning controllability [3].

Case 3 The manifold of Eq. (4) is $S3 = \emptyset$. The system cannot be controlled in this case. We do not discuss the case in this paper.

Note that $(-\infty, \alpha_1)$ is a particular case of (α_1, α_2). In the following, we mainly discuss the case (α_1, α_2) and the conclusion is also applicable for the case $(-\infty, \alpha_1)$. Besides, the synchronization manifolds of the three cases characterize the candidate range of β and depend on the nodal dynamics and the coupling matrix. However, the manifolds are irrelevant to the network structure and the determination of the pinning

nodes. The selection of pinning nodes would influence the eigenvalues λ_k of $-L-D$ that is reflected by $\beta = c\lambda_k$ in Eq. 4. In the following part, we focus on the relationship between the selection of pinning nodes and λ_k.

2.3 The coupling range and convergence speed

The coupling range To control a network, we usually desire a convenient strategy to tune the coupling strength between nodes, which means that a wider range of the candidate coupling strength is better. Intuitively, a larger R implies larger $\alpha_1$and smaller α_2, which corresponds to a wider range of the coupling strength. However, there is no strict relationship between R and the range of the coupling strength. The strict range of the coupling strength ('coupling range' for short) is characterized by

$$\omega = \frac{\alpha_1}{\lambda_N} - \frac{\alpha_2}{\lambda_1}. \tag{8}$$

For a fixed number m of pinning nodes, we should optimize the following objective function,

$$\max \quad \omega, \tag{9}$$

which subjects to

$$\frac{1}{d}\mathbf{1}^T D\mathbf{1} = m, \quad D_{ii} \in \{0, d\}, \tag{10}$$

where $\mathbf{1} = [1, 1, \ldots, 1]^T_{N\times 1}$ is an identity vector. Equation (10) guarantees that we choose a fixed number m of pinning nodes, and a node is either a pinning node or not. Here, we treat all pinning nodes have identical feedback gains.

Note that R and the coupling range ω have completely different formalisms. R cannot accurately represent ω in characterizing the range of the coupling strength.

The convergence speed When controlling a network, another concern is how to increase (or decrease) the convergence rate of the pinning system (or Lyapunov exponent). The strict convergence rate of nodal states is characterized by the largest eigenvalue of $(Df + c\lambda_i H^T)$, denoted as $\Lambda_{\max}[Df + c\lambda_i H^T]$, which are relevant to all λ_i, $i = 1, 2, .., N$. In the standard control theory, $\Lambda_{\max}[Df + c\lambda_i H^T]$ is also the Lyapunov exponent of the system. In many real scenarios, the function $\Lambda_{\max}[Df + \beta H^T]$ only has one minimal point as a function of β, such as Lorenz attractor [45], Rössler attractor [46], Chen attractor [47,48], and many other kinds of nodal dynamics [49]. Thus, the convergence speed of the pinning system is simplified by the largest eigenvalues of $(Df + c\lambda_1 H^T)$ and $(Df + c\lambda_N H^T)$ as

$$v = \max\{\Lambda_{\max}[Df + c\lambda_1 H^T], \Lambda_{\max}[Df + c\lambda_N H^T]\}. \tag{11}$$

v is also the Lyapunov exponent of Eq. (2). For a fixed number m of pinning nodes, we should optimize the following objective function,

$$\min \quad v, \tag{12}$$

which also subjects to Eq. (10). Note that when optimizing v, $v < 0$ means the network could be controlled by the control strategies. A smaller v indicates higher speed of convergence (smaller Lyapunov exponent) and is better, whereas $v > 0$ means that the network cannot be controlled.

2.4 The difference among ratio metric, coupling range and convergence speed

The ratio metric, coupling range and convergence speed have completely different formalisms [see Eqs. (7), (8) and (11)]. However, previous work roughly utilizes the ratio metric to evaluate the pinning controllability. Given a set of driver nodes, the problem of how the driver nodes influence the three metrics remains unclear. Since the three metrics are mainly determined by the largest and the smallest eigenvalues of $-L-D$, we investigate the selection of pinning nodes on the two eigenvalues of $-L-D$. In the part, based on perturbation theory, we analytically derive the influence of pinning nodes on the three metrics.

Lemma 1 [50,51] *Supposing that we apply feedback gains to a small fraction of nodes with the feedback strength d_i (In Eq. (2), $d_i \in \{0, d\}$), and denoting χ_k as the eigenvector that corresponds to the eigenvalue λ_k of $-L$, $|\chi_k| = 1$. After pinning a small fraction of nodes, the eigenvalues λ'_k of $-L-D$ could be evaluated as*

$$\lambda'_k \approx \lambda_k - \chi_k^T D\chi_k. \tag{13}$$

Proof Denoting $\chi'_k = \chi_k + \Delta\chi_k$ as the eigenvector that corresponds to the eigenvalue λ'_k of $-L-D$, λ'_k and χ'_k satisfy

$$(-L - D)(\chi_k + \Delta\chi_k) = (\lambda_k + \Delta\lambda_k)(\chi_k + \Delta\chi_k). \tag{14}$$

Left-multiplying Eq. (14) by χ_k^T, we obtain

$$-\chi_k^T D\chi_k - \chi_k^T D\Delta\chi_k = \Delta\lambda_k \chi_k^T \chi_k + \Delta\lambda_k \chi_k^T \Delta\chi_k. \tag{15}$$

Neglecting the second-order terms $\chi_k^T D\Delta\chi_k$ and $\Delta\lambda_k \chi_k^T \Delta\chi_k$, we have [32,50]

$$\Delta\lambda_k \approx -\frac{\chi_k^T D\chi_k}{\chi_k^T \chi_k} = -\chi_k^T D\chi_k. \tag{16}$$

where $\chi_k^T \chi_k = 1$. For more details about the proof, please refer to refs. [32,50,51]. □

Since D is a diagonal matrix, we rewrite Eq. (16) in a different formalism,

$$\Delta\lambda_k \approx -\sum_i d_i (\chi_k^i)^2, \tag{17}$$

where χ_k^i is the i th element of the eigenvector χ_k. Note that the fluctuation $\Delta\lambda_k$ of λ_k induced by pinning strategies is the sum of $(\chi_k^i)^2$ for the whole pinning nodes and the other nodes ($d_i = 0$) contribute none to the $\Delta\lambda_k$. Thus, we arrive at the partial differential of λ_k on the feedback strength of node i [32],

$$\frac{\partial\lambda_k}{\partial d_i} = \lim_{d_i\to\infty} \frac{\Delta\lambda_k}{d_i} = -(\chi_k^i)^2. \tag{18}$$

Based on Eqs. (7) and (18), the variation of the ratio controllability is

$$\begin{aligned}\frac{\partial R}{\partial d_i} &= \frac{\partial}{\partial d_i}\left(\frac{\lambda_1}{\lambda_N}\right) = \frac{\lambda_N \frac{\partial\lambda_1}{\partial d_i} - \lambda_1 \frac{\partial\lambda_N}{\partial d_i}}{\lambda_N^2} \\ &= -\frac{1}{\lambda_N}\left[\left(\chi_1^i\right)^2 - R\left(\chi_N^i\right)^2\right].\end{aligned} \tag{19}$$

The variation of the coupling range is

$$\begin{aligned}\frac{\partial\omega}{\partial d_i} &= \frac{\partial}{\partial d_i}\left(\frac{\alpha_1}{\lambda_N} - \frac{\alpha_2}{\lambda_1}\right) = -\left(\frac{\alpha_1}{\lambda_N^2}\frac{\partial\lambda_N}{\partial d_i} - \frac{\alpha_2}{\lambda_1^2}\frac{\partial\lambda_1}{\partial d_i}\right) \\ &= \frac{\alpha_1}{\lambda_N^2}\left(\chi_N^i\right)^2 - \frac{\alpha_2}{\lambda_1^2}\left(\chi_1^i\right)^2.\end{aligned} \tag{20}$$

Accordingly, the variation of the convergence speed is

$$\frac{\partial v}{\partial d_i} = \begin{cases} -c\frac{\partial F(\rho)}{\partial\rho}(\chi_1^i)^2, & F(c\lambda_1) > F(c\lambda_N), \\ -c\frac{\partial F(\rho)}{\partial\rho}(\chi_N^i)^2, & F(c\lambda_1) < F(c\lambda_N), \\ \max\left\{-c\frac{\partial F(\rho)}{\partial\rho}(\chi_1^i)^2, -c\frac{\partial F(\rho)}{\partial\rho}(\chi_N^i)^2\right\}, & \text{otherwise}, \end{cases} \tag{21}$$

where $F(\rho) = \Lambda_{\max}[Df + \rho H^T]$.

From the variation formalisms of the ratio controllability [Eq. (19)], coupling range [Eq. (20)] and convergence speed [Eq. (21)], we see that pinning a node contributes to R, ω and v differently and the three metrics characterize the pinning controllability from different perspectives. The increase in one metric may induce the decrease in another metric. Thus, we cannot guarantee the optimums of the three metrics simultaneously, which is validated in Fig. 1 and the experimental results.

3 Results

In the section, we first describe the five networks used in the experiments and then show the performance of the three metrics.

3.1 Dataset description

To verify the effectiveness of the proposed method, we measure the performance of our framework in five empirical networks from diverse disciplines and backgrounds: (1) PDZBase [52]: An undirected network of protein–protein interactions from PDZBase. (2) Italy PowerGrid network [53]: This undirected network contains information about the power grid of Italy. An edge represents a power supply line. A node is either a generator, a transformator or a substation. (3) US Air [50]: A directed network of flights between US airports in 2010. Each link represents a connection from one airport to another in 2010. (4) Neural [50]: A directed and weighted neural network of C.elegans. (5) Karate [54]: The Zachary karate club network was collected from an university karate club by Wayne Zachary in 1977. Each node represents a member of the club, and each edge represents a relationship between two members.

Different real networks contain directed or undirected, weighted or unweighted links. To simplify the problem, we treat all links undirected and unweighted. Besides, only the giant connected components of these networks are taken into account. This is because that distinct clusters can be treated as independent subnetworks, which means that different networks are investigated simultaneously. Table 1 shows the basic statistics of those networks.

Table 1 Structural properties of the different real networks

Network	N	E	H	r	$< C >$	$< d >$	Sparsity
Italy PowerGrid	67	93	1.158	−0.036	0.022	6.70	3.0×10^{-2}
PDZBase	161	209	2.263	−0.466	0.001	5.11	1.6×10^{-2}
US Air	332	2126	3.464	−0.208	0.625	2.74	3.9×10^{-2}
Neural	297	2148	1.81	−0.163	0.292	2.46	4.9×10^{-2}
Karate	34	78	1.69	−0.475	0.074	2.41	0.139

Structural properties include network size (N), edge number (E), degree heterogeneity ($H =< k^2 > / < k >^2$), degree assortativity (r), average clustering coefficient ($< C >$), average shortest path length ($< d >$) and sparsity

3.2 Experimental results

Equation (1) represents a general dynamics of various systems. Without loss of generality, in our experiments, we use Rössler oscillator as the nodal dynamics that follows

$$\begin{aligned} \dot{x}_{i1} &= -(x_{i2} + x_{i3}), \\ \dot{x}_{i2} &= x_{i1} + a_1 x_{i2}, \\ \dot{x}_{i3} &= a_2 + x_{i3}(x_{i1} - a_3), \end{aligned} \tag{22}$$

where $\mathbf{x}_i = (x_{i1}, x_{i2}, x_{i3})^T$, and a_1, a_2 and a_3 are three parameters. We consider two kinds of parameter settings: (1) Case 1 (used in Figs. 1, 2, 3, 4, 5), we set $a_1 = 0.2$, $a_2 = 0.4$ and $a_3 = 5.7$. The coupling matrix is $H = \text{diag}\{1, 0, 0\}$. A stationary point of the dynamics is $\bar{\mathbf{x}} = (0.014, -0.070, 0.070)^T$. The coupling strength is $c = 0.3$. The aim is to drive the network to the stationary state $\bar{\mathbf{x}}$. Accordingly, the manifold is $(\alpha_1, \alpha_2) = (-4.98, -0.19)$. (2) Case 2 (Only used in Fig. 6), we set $a_1 = 0.9$ and the other parameters are the same with that of case 1. We argue that the results and conclusions still hold and are not limited to the particular nodal dynamics and the particular parameters introduced above.

Figure 2 shows the ratio R as a function of the size of pinning node sets that correspond to the optimal R, ω and v, respectively. For the four real networks, the optimal pinning nodes of ω and v cannot arrive at the maximal R regardless of the size of pinning nodes, especially in Fig. 2b, implying that the three metrics do not agree with each other in some practical scenarios. The results agree well with theoretical analysis in Sect. 2.4 that the three metrics are completely different. Note that the optimal R is in accordance with ω, while v diverges from the other two metrics, which is due to the particular case of the network structure and parameter settings. In Fig. 6, we show the divergence of R and ω.

Apart from the ratio R, we also show the performances ω and v as a function of the size of pinning node sets by optimizing R, ω and v, respectively, in Figs. 3 and 4. In the two figures, v diverges from the other two metrics obviously, while R and ω are in accordance with either with small difference except at some particular points, $\delta = 0.36$ in Fig. 3a, $\delta = 0.04$ in Fig. 3b, $\delta = 0.18$ in Fig. 4a and that in Fig. 4b. The consistency between R and ω is due to the particular networks and parameters that is explained in Fig. 6. Figures 3 and 4 further demonstrate the differences among R, ω and v, which indicates that optimizing a single objective metric cannot reach the optimums of the three metrics simultaneously. Note that according to Fig. 4, optimizing R and ω cannot guarantee the control of the system, since the optimal R and ω possess $v > 0$ in many cases. $v > 0$ means positive Lyapunov exponent and the system is chaotic. Another notice is that larger R usually implies larger ω and smaller v. However, the optimal R indicates neither the optimal coupling range nor the highest convergence speed. Consequently, R cannot characterize the pinning controllability precisely. By contrast, ω and v evaluate either the coupling range or the convergence speed accurately.

Moreover, since R agrees well with ω in Figs. 2, 3, and 4, we investigate the overlap of the pinning sets of the three different metrics. The overlap is characterized by the hub depressed index (HDI) [55],

$$\text{HDI}_{R,\omega} = \frac{|\Gamma(R) \bigcap \Gamma(\omega)|}{\max\{|\Gamma(R)|, |\Gamma(\omega)|\}}, \tag{23}$$

where $\Gamma(R)$ and $\Gamma(\omega)$ are the sets of pinning nodes calculated by optimizing R and ω. $|\ldots|$ is the size of the set. We fix $|\Gamma(R)| = |\Gamma(\omega)|$. $\text{HDI}_{R,\omega}$ ranges from 0 to 1. $\text{HDI}_{R,\omega} \to 0$ indicates completely different pinning

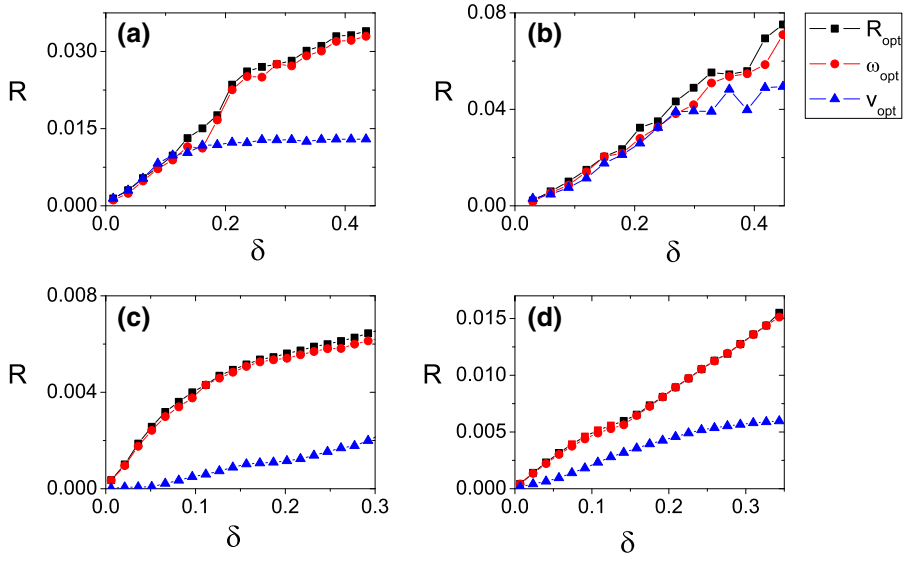

Fig. 2 The ratio metric R as a function of the size of pinning nodes and the different optimizing schemes. R_{opt}, ω_{opt} and v_{opt} represent the results of the optimal pinning node sets obtained by optimizing R, ω and v, respectively. $\delta = m/N$ is the fraction of the pinning nodes. **a** Italy PowerGrid network. **b** PDZBase network. **c** US Air network. **d** Neural network

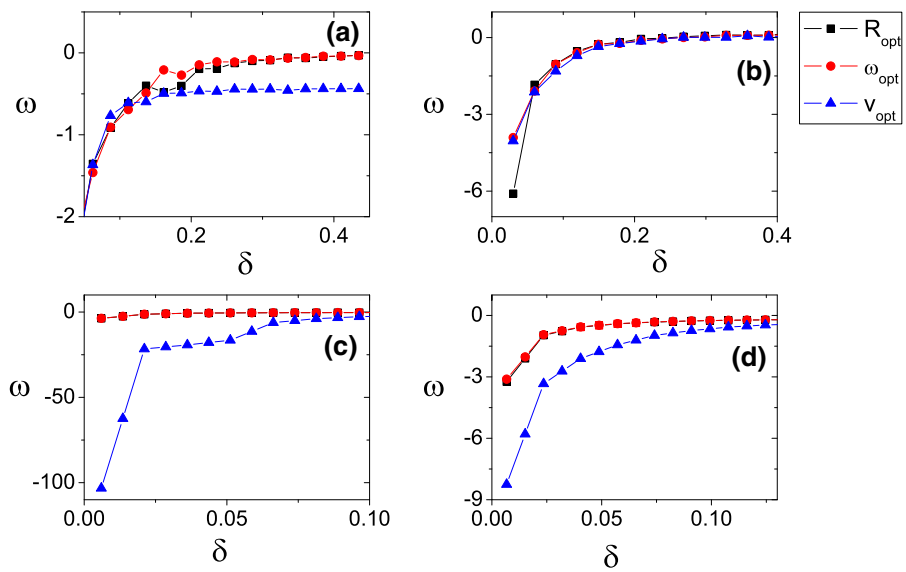

Fig. 3 The coupling range ω as a function of the size of pinning nodes and the different optimizing schemes. R_{opt}, ω_{opt} and v_{opt} represent the results of the optimal pinning node sets obtained by optimizing R, ω and v, respectively. $\delta = m/N$ is the fraction of the pinning nodes. **a** Italy PowerGrid network. **b** PDZBase network. **c** US Air network. **d** Neural network

nodes of R and ω, while $\text{HDI}_{R,\omega} \to 1$ means that the two metrics choose almost the same set of pinning nodes. Accordingly, the overlaps $\text{HDI}_{R,v}$ and $\text{HDI}_{\omega,v}$ could also be defined as Eq. (23).

Figure 5 shows the overlaps $\text{HDI}_{R,\omega}$, $\text{HDI}_{R,v}$ and $\text{HDI}_{\omega,v}$. In Fig. 5, the three overlaps in the four networks are small except $\text{HDI}_{R,\omega}$. Then, we compare the sets of pinning nodes by optimizing R and ω, and find that the two metrics achieve a large fraction of common pinning nodes in US Air and Neural networks, resulting in their similar performance in Figs. 2, 3 and 4.

Lastly, we explain that R may also diverge from ω, which is different from Figs. 2, 3 and 4. We turn to the second case of the parameter settings (in the beginning of the Sect. 3.2). Figure 6 shows the three metrics (R, ω and v) as a function of the size of pinning nodes that correspond to the optimal three metrics, respectively. The three metrics diverge from each other obviously. Besides, for many other parameter settings, we can also observe the difference of the three metrics. Moreover, we have also applied other nodal dynamics (such as Lorentz oscillator and Chen oscillator) to the three metrics. The results show that the differences between the three metrics largely exist in various scenarios and are similar to Figs. 2, 3, 4, 5 and 6, which further illus-

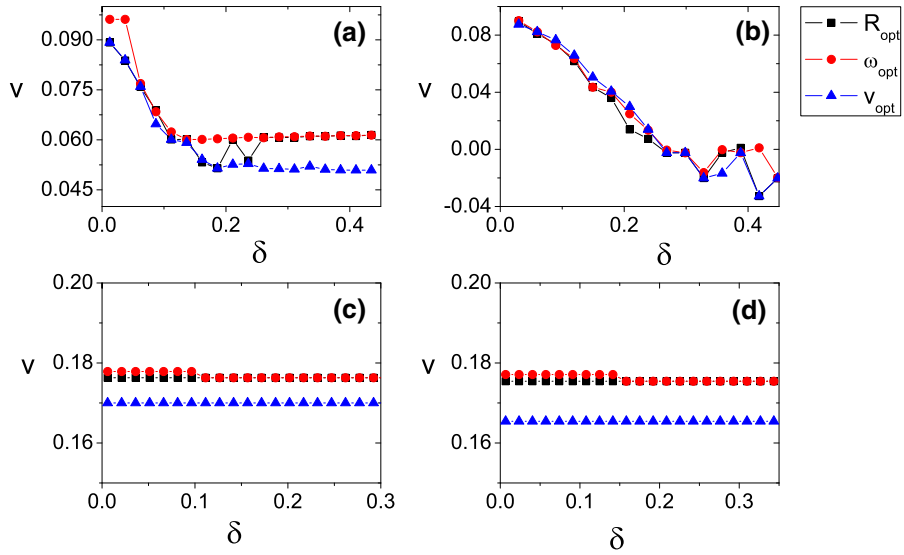

Fig. 4 The convergence speed v as a function of the size of pinning nodes and the different optimizing schemes. R_{opt}, ω_{opt} and v_{opt} represent the results of the optimal pinning node sets obtained by optimizing R, ω and v, respectively. $\delta = m/N$ is the fraction of the pinning nodes. **a** Italy PowerGrid network. **b** PDZBase network. **c** US Air network. **d** Neural network

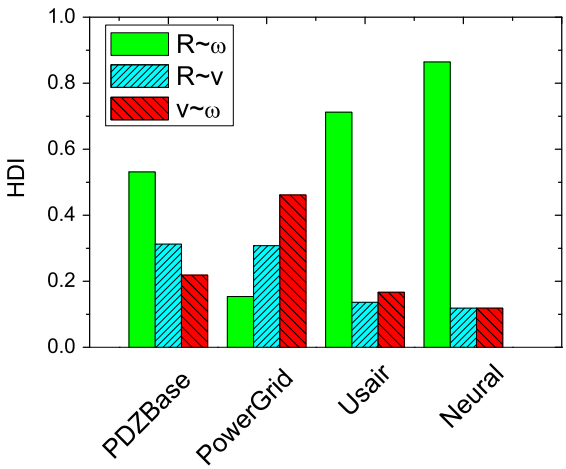

Fig. 5 The intersection between the different sets of pinning nodes of the three metrics. In the figure, we calculate 20% optimal pinning nodes for each metric. $R \sim \omega$ means the intersection between the optimal pinning nodes of R and ω metrics. $R \sim v$ and $v \sim \omega$ follow the similar definition of $R \sim \omega$

trates the drawback of R and the effectiveness of the proposed ω and v.

Based on the experiments introduced above, we conduct that the three metrics perform differently in real networks. The results further illustrate the validity of the analytical results in Sect. 2.4 that the three metrics characterize pinning controllability from different perspectives. ω describes the coupling range, while v describes the Lyapunov exponent. However, the classical R only roughly characterizes ω and v, lacking high precision.

4 Conclusion

In conclusion, we investigate the metrics to characterize the pinning controllability in complex networks. We find that the state-of-the-art eigenvalue-based ratio metric cannot fully characterize the pinning controllability. To solve this issue, we propose two metrics to better describe the pinning controllability: One is coupling range, and the other one is convergence speed. Besides, we utilize the differential evolution method to optimize the classical ratio metric, coupling range and convergence speed in real networks. The results show that optimizing one metric cannot guarantee the optimums of the other two metrics. The two proposed metrics could better characterize the coupling range and convergence rate than the ratio metric.

Our work enhances our understanding of the pinning control problem. In the field of control engineering, for example, when designing the strategies to control a flock of unmanned aerial vehicles, we desire easy access to tuning the coupling strength that is relevant to the distance between vehicles, the range of the coupling strength should be maximized; while if we want to increase (decrease) the convergence rate (Lyapunov exponent), we should optimize the convergence speed. Thus, a better control could be achieved by balancing the coupling range and convergence speed in

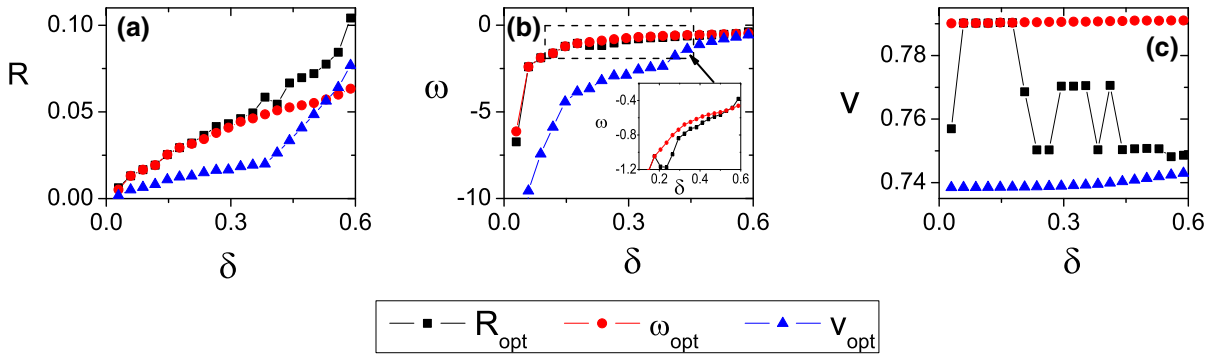

Fig. 6 **a** The ratio metric R as a function of the size ($\delta = m/N$) of pinning nodes. **b** The coupling range ω as a function of the size of pinning nodes. **c** The convergence speed v as a function of the size of pinning nodes. The parameters are shown in Sect. 3.2. R_{opt}, ω_{opt} and v_{opt} represent the optimal pinning node sets obtained by optimizing R, ω and v, respectively

networked systems. Besides, comparing with the ratio metric, calculating the coupling range and convergence speed requires higher time complexity. Future works are to design better accurate metrics to describe the pinning controllability and reduce the time complexity when calculating the coupling range and convergence speed.

Acknowledgements The authors acknowledge Dr. Alexandre Vidmer for helping improve the quality of the manuscript. This work was jointly supported by the National Natural Science Foundation of China (Nos. 61703281, 11547040, 61803266, 61503140 and 61873171), the Ph.D. Start-Up Fund of Natural Science Foundation of Guangdong Province, China (Nos. 2017A030310374 and 2016A030313036), the Science and Technology Innovation Commission of Shenzhen (No. JCYJ20160520 162743717), Shenzhen Science and Technology Foundation (Nos. JCYJ20150529164656096 and JCYJ20170302153955 969), Guangdong Pre-national project (2014GKXM054), Guangdong Province Key Laboratory of Popular High Performance Computers (2017B030314073), Foundation for Distinguished Young Talents in Higher Education of Guangdong (2015KONCX 143), and the Young Teachers Start-up Fund of Natural Science Foundation of Shenzhen University.

Compliance with ethical standards

Conflicts of interest The authors declared that they have no conflict of interest.

References

1. Wang, X., Li, X., Jinhu, L.: Control and flocking of networked systems via pinning. IEEE Circuits Syst. Mag. **10**(3), 83–91 (2010)
2. Olfati-Saber, R.: Flocking for multi-agent dynamic systems: algorithms and theory. IEEE Trans. Autom. Control **51**(3), 401–420 (2006)
3. Liu, Y.-Y., Barabási, A.-L.: Control principles of complex systems. Rev. Mod. Phys. **88**(3), 035006 (2016)
4. Pecora, L.M., Carroll, T.L.: Master stability functions for synchronized coupled systems. Phys. Rev. Lett. **80**(10), 2109 (1998)
5. Stankovski, T., Pereira, T., McClintock, P.V.E., Stefanovska, A.: Coupling functions: universal insights into dynamical interaction mechanisms. Rev. Mod. Phys.cs **89**(4), 045001 (2017)
6. Yang, W., Wang, Y., Wang, X., Shi, H., Ou, L.: Optimal selection strategy for multi-agent system with single leader. In: CDC, pp. 2767–2772 (2012)
7. Yan, G., Vértes, P.E., Towlson, E.K., Chew, Y.L., Walker, D.S., Schafer, W.R., Barabási, A.-L.: Network control principles predict neuron function in the caenorhabditis elegans connectome. Nature **550**(7677), 519 (2017)
8. Wen-Bo, D., Ying, W., Yan, G., Zhu, Y.-B., Cao, X.-B.: Heterogeneous strategy particle swarm optimization. IEEE Trans. Circuits Syst. II: Express Br. **64**(4), 467–471 (2017)
9. Tang, Y., Qian, F., Gao, H., Kurths, J.: Synchronization in complex networks and its application—a survey of recent advances and challenges. Annu. Rev. Control **38**(2), 184–198 (2014)
10. Arenas, A., Diaz-Guilera, A., Kurths, J., Moreno, Y., Zhou, C.: Synchronization in complex networks. Phys. Rep. **469**(3), 93–153 (2008)
11. Xiang, L.Y., Liu, Z.X., Chen, Z.Q., Chen, F., Yuan, Z.Z.: Pinning control of complex dynamical networks with general topology. Phys. A: Stat. Mech. Appl. **379**(1), 298–306 (2007)
12. Li, X., Wang, X., Chen, G.: Pinning a complex dynamical network to its equilibrium. IEEE Trans. Circuits Syst. I: Regul. Pap. **51**(10), 2074–2087 (2004)
13. Wang, X., Housheng, S.: Pinning control of complex networked systems: a decade after and beyond. Annu. Rev. Control **38**(1), 103–111 (2014)

14. Bao, H., Park, J.H., Cao, J.: Adaptive synchronization of fractional-order memristor-based neural networks with time delay. Nonlinear Dyn. **82**(3), 1343–1354 (2015)
15. Guan, Z.-H., Liu, Z.-W., Feng, G., Wang, Y.-W.: Synchronization of complex dynamical networks with time-varying delays via impulsive distributed control. IEEE Trans. Circuits Syst. I: Regul. Pap. **57**(8), 2182–2195 (2010)
16. Cowan, N.J., Chastain, E.J., Vilhena, D.A., Freudenberg, J.S., Bergstrom, C.T.: Nodal dynamics, not degree distributions, determine the structural controllability of complex networks. PloS ONE **7**(6), e38398 (2012)
17. Nepusz, T., Vicsek, T.: Controlling edge dynamics in complex networks. Nat. Phys. **8**(7), 568 (2012)
18. Amani, A.M., Jalili, M., Xinghuo, Y., Stone, L.: Finding the most influential nodes in pinning controllability of complex networks. IEEE Trans. Circuits Syst. II: Express Br. **64**(6), 685–689 (2017)
19. He, W., Zhang, B., Han, Q.-L., Qian, F., Kurths, J., Cao, J.: Leader-following consensus of nonlinear multiagent systems with stochastic sampling. IEEE Trans. Cybern. **47**(2), 327–338 (2017)
20. Wang, X., She, K., Zhong, S., Cheng, J.: Synchronization of complex networks with non-delayed and delayed couplings via adaptive feedback and impulsive pinning control. Nonlinear Dyn. **86**(1), 165–176 (2016)
21. Guo, L., Cao, S.: Anti-disturbance control theory for systems with multiple disturbances: a survey. ISA Trans. **53**(4), 846–849 (2014)
22. He, W., Chen, G., Han, Q.-L., Qian, F.: Network-based leader-following consensus of nonlinear multi-agent systems via distributed impulsive control. Inf. Sci. **380**, 145–158 (2017)
23. Xing, L., Wen, C., Liu, Z., Hongye, S., Cai, J.: Event-triggered adaptive control for a class of uncertain nonlinear systems. IEEE Trans. Autom. Control **62**(4), 2071–2076 (2017)
24. Wang, L., Dai, H.P., Dong, H., Cao, Y.Y., Sun, Y.X.: Adaptive synchronization of weighted complex dynamical networks through pinning. Eur. Phys. J. B **61**(3), 335–342 (2008)
25. Song, Q., Cao, J.: On pinning synchronization of directed and undirected complex dynamical networks. IEEE Trans. Circuits Syst. I: Regul. Pap. **57**(3), 672–680 (2010)
26. Lei, X., Cai, S., Jiang, S., Liu, Z.: Adaptive outer synchronization between two complex delayed dynamical networks via aperiodically intermittent pinning control. Neurocomputing **222**, 26–35 (2017)
27. Porfiri, M., Pigliacampo, R.: Master-slave global stochastic synchronization of chaotic oscillators. SIAM J. Appl. Dyn. Syst. **7**(3), 825–842 (2008)
28. DeLellis, P., Garofalo, F., Porfiri, M., et al.: Evolution of complex networks via edge snapping. IEEE Trans. Circuits Syst. I: Regul. Pap. **57**(8), 2132–2143 (2010)
29. DeLellis, P., Garofalo, F., Iudice, F.L.: The partial pinning control strategy for large complex networks. Automatica **89**, 111–116 (2018)
30. Barabási, A.-L.: Network Science. Cambridge University Press, Cambridge (2016)
31. Ducruet, C., Beauguitte, L.: Spatial science and network science: review and outcomes of a complex relationship. Netw. Spat. Econ. **14**(3–4), 297–316 (2014)
32. Jalili, M., Xinghuo, Y.: Enhancing pinning controllability of complex networks through link rewiring. IEEE Trans. Circuits Syst. II: Express Br. **64**(6), 690–694 (2017)
33. Yang, W., Cao, L., Wang, X., Li, X.: Consensus in a heterogeneous influence network. Phys. Rev. E **74**(3), 037101 (2006)
34. Liao, H., Mariani, M.S., Medo, M., Zhang, Y.-C., Zhou, M.-Y.: Ranking in evolving complex networks. Phys. Rep. **689**, 1–54 (2017)
35. Chen, G.: Pinning control and controllability of complex dynamical networks. Int. J. Autom. Comput. **14**(1), 1–9 (2017)
36. Kitsak, M., Gallos, L.K., Havlin, S., Liljeros, F., Muchnik, L., Stanley, H.E., Makse, H.A.: Identification of influential spreaders in complex networks. Nat. Phys. **6**(11), 888–893 (2010)
37. Wang, X.F., Chen, G.: Pinning control of scale-free dynamical networks. Phys. A: Stat. Mech. Appl. **310**(3–4), 521–531 (2002)
38. Rong, Z. H., Li, X., Lu, W. L.: Pinning a complex network through the betweenness centrality strategy. In: IEEE International Symposium on Circuits and Systems, 2009. ISCAS 2009. IEEE, pp. 1689–1692 (2009)
39. Jalili, M., Sichani, O.A., Xinghuo, Y.: Optimal pinning controllability of complex networks: dependence on network structure. Phys. Rev. E **91**(1), 012803 (2015)
40. Orouskhani, Y., Jalili, M., Xinghuo, Y.: Optimizing dynamical network structure for pinning control. Sci. Rep. **6**, 24252 (2016)
41. Barabási, A.-L.: Network science. Philos. Trans. R. Soc. A **371**(1987), 20120375 (2013)
42. Fortunato, S., Hric, D.: Community detection in networks: a user guide. Phys. Rep. **659**, 1–44 (2016)
43. Wenlian, L., Chen, T.: New approach to synchronization analysis of linearly coupled ordinary differential systems. Phys. D: Nonlinear Phenom. **213**(2), 214–230 (2006)
44. Wenwu, Y., Chen, G., Jinhu, L., Kurths, J.: Synchronization via pinning control on general complex networks. SIAM J. Control Optim. **51**(2), 1395–1416 (2013)
45. Stewart, I.: Mathematics: the Lorenz attractor exists. Nature **406**(6799), 948 (2000)
46. Rössler, O.E.: An equation for continuous chaos. Phys. Lett. A **57**(5), 397–398 (1976)
47. Lü, J., Chen, G.: A new chaotic attractor coined. Int. J. Bifurc. Chaos **12**(03), 659–661 (2002)
48. Chen, G., Ueta, T.: Yet another chaotic attractor. Int. J. Bifurc. Chaos **9**(07), 1465–1466 (1999)
49. Williams, G.: Chaos Theory Tamed. CRC Press, Boca Raton (2014)
50. Lü, L., Pan, L., Zhou, T., Zhang, Y.-C., Stanley, H.E.: Toward link predictability of complex networks. Proc. Natl. Acad. Sci. **112**(8), 2325–2330 (2015)
51. Stewart, G.W.: Matrix Perturbation Theory. Academic Press, New York (1990)
52. Beuming, T., Skrabanek, L., Niv, M.Y., Mukherjee, P., Weinstein, H.: Pdzbase: a protein–protein interaction database for pdz-domains. Bioinformatics **21**(6), 827–828 (2004)
53. Motter, A.E., Myers, S.A., Anghel, M., Nishikawa, T.: Spontaneous synchrony in power-grid networks. Nat. Phys. **9**(3), 191 (2013)

54. Zachary, W.W.: An information flow model for conflict and fission in small groups. J. Anthropol. Res. **33**(4), 452–473 (1977)
55. Lü, L., Zhou, T.: Link prediction in complex networks: a survey. Phys. A: Stat. Mech. Appl. **390**(6), 1150–1170 (2011)